18th Brazilian Congress of Thermal Sciences and Engineering
November 16-20, 2020 (Online)

ENC-2020-0430
SIMULATION OF SUPERSONIC FLOW OVER A CONE WITH THE SU2 CODE: VERIFICATION AND VALIDATION

Dener Augusto Iorio
Postgraduate Program in Mechanical Engineering (PGMEC), Federal University of Paraná (UFPR), Curitiba, PR, Brazil
dener.iorio@ufpr.br

Guilherme Bertoldo
Department of Physics, Statistics and Mathematics (DAFEM), Federal University of Technology – Paraná (UTFPR), Campus Francisco Beltrão, ZIP Code 85601-970, Francisco Beltrão, PR, Brazil
gbertoldo@utfpr.edu.br

Carlos Henrique Marchi
Laboratory of Numerical Experimentation (LENA), Department of Mechanical Engineering (DEMEC), Federal University of Paraná (UFPR), P.O. Box 19040, ZIP Code 81531-980, Curitiba, PR, Brazil
chmcfd@gmail.com

Abstract. *The verification of the numerical solution of Euler's mathematical model present in the SU2 code and the validation of this mathematical model for an external flow problem are objectives of this work. The problem of a cone, with fineness ratio three, subject to a supersonic flow with Mach number 3.50 was addressed. Simulations were performed using up to eight meshes, with 20x20 to 2560x2560 volumes. The drag coefficients obtained from the simulations and ones calculated using extrapolated wall pressure distribution were compared with the numerical solution of the Taylor-Maccoll flow, with the numerical solution of another computational code and with experimental results. Furthermore, this work presents estimates of the numerical error and extrapolated numerical solutions with the Repeated Richardson Extrapolation method and the convergent solution. The GCI estimator presented the most conservative estimate, indicating that the estimated numerical error range of the numerical solution of the finest simulated mesh is 0.002% of its value. The validation indicated that using Euler's mathematical model to represent the phenomenon results in a modeling error estimate in the range of -9.16% to -4.47% of the experimental result.*

Keywords: *SU2, cone, verification, validation, CFD*

1. INTRODUCTION

Verification and validation are procedures used to measure with which level of fidelity a numerical solution represents a physical phenomenon. These are important procedures for the evaluation of numerical flow simulation codes, since, in general, due to the complex mathematical models it is only possible to obtain numerical results for fluid dynamics problems.

This work performes the verification of the numerical solution of Euler's mathematical model implemented in the SU2 code (Economon et al., 2016) for the problem of supersonic air flow over a cone and the validation of this mathematical model according to the procedure defined by the ASME V&V 20-2009 standard. The variable of interest is the drag coefficient. For this variable of interest, it will be presented estimates of numerical error and solutions extrapolated with Repeated Richardson Extrapolation (RRE) (Marchi et al., 2013) and the convergent solution (Marchi and Silva, 2002). It will also be presented the use of a method of extrapolating properties to reduce the difference of the drag coefficient with the reference values.

Other authors have already submitted proposals for verification and validation of the SU2 code, but these have focused on the mathematical models of Navier-Stokes (Van der Weide and Economon, 2019) and turbulence models (Castro, 2019; Mishra et al., 2019; Becker and Granzoto, 2018; Keep et al., 2017; Palacios et al., 2014). However, the numerical error was not estimated by most of these authors. Generally, these works present studies of convergence of the solution with the refinement of the mesh (Castro, 2019; Becker and Granzoto, 2018) and comparisons, usually graphical, with experimental results or other consolidated codes (Castro, 2019; Mishra et al., 2019; Becker and Granzoto, 2018; Keep et al., 2017; Palacios et al., 2014). Only two research were found that studied the effective order or the apparent order of the numerical error (Van der Weide and Economon, 2019; Castro, 2019) and two that presented estimates of numerical error (Castro, 2019; Mishra et al., 2019).

2. METHODOLOGY

The methodology used in the verification and validation consists in the simulation of the supersonic flow over a cone in different meshes and subsequent analysis of errors, making error estimates and comparing the numerical solution of the variable of interest with the results by other methods. This section presents the definition of the problem and the verification and validation procedure.

2.1 Definition of the problem

The fluid dynamics problem that will be addressed in this work consists of supersonic flow of air over a cone, as illustrated in Fig. 1, where L is the length of the cone, r_b is its base radius, M is the Mach number of the flow and the arrows parallel to the x axis indicate the flow direction. The flow properties and the geometric characteristics of the cone are based on the experimental study by Eggers Junior et al. (1957). Table 1 shows the data used for the free-stream Mach number M_∞, temperature T_∞, the ratio of specific heats γ_∞ and pressure p_∞, along with the length L and base radius r_b of the cone. The fineness ratio is the ratio between the length and the base diameter of the cone.

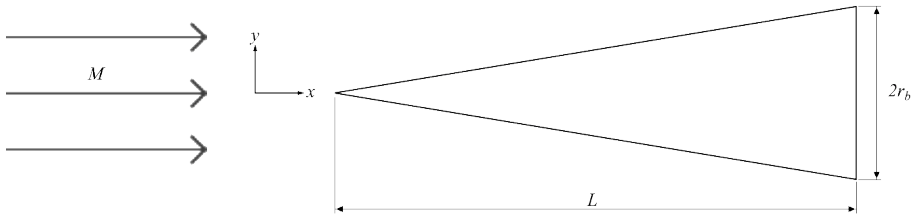

Figure 1. Illustration of the problem.

Table 1. Geometric and flow properties.

Parameter	Value
Cone length	0.0762 m (3 in)
Base radius	0.0127 m (0.5 in)
Fineness ratio	3
Mach number	3.50
Axial velocity	1215.3 m/s
Temperature	300 K
Ratio of specific heats	1.40
Gas constant	287.058 J/kg.K
Pressure	607950 Pa

The flow was considered as inviscid, compressible, adiabatic and axisymmetric. Thereby it is mathematically modeled by Euler's equations in its two-dimensional axisymmetric form. Euler equations can be represented by (Hirsch, 2007)

$$\frac{\partial \mathbf{U}}{\partial t} + \nabla \cdot \mathbf{F}^c(\mathbf{U}) = 0 \tag{1}$$

where t is time, $\mathbf{U}$ is the vector of conservative variables and $\mathbf{F}^c$ is the advective flux, represented by

$$\mathbf{U} = \begin{Bmatrix} \rho \\ \rho \mathbf{v} \\ \rho E \end{Bmatrix}, \quad \mathbf{F}^c = \begin{Bmatrix} \rho \mathbf{v} \\ \rho \mathbf{v} \otimes \mathbf{v} + \bar{\mathbf{I}} p \\ \rho E \mathbf{v} + p \mathbf{v} \end{Bmatrix} \tag{2}$$

where ρ means the density of the fluid, $\mathbf{v}$ is the velocity vector with components axial u and radial v, and E is the total energy per unit mass. Moreover, p is the pressure, $\bar{\mathbf{I}}$ is a 2x2 identity matrix and $\otimes$ represents the tensor product.

The Euler's system of equations express the conservation of mass, the conservation of momentum and the conservation of total energy. In order to close the system of equations, the polytropic gas equation (Hughes et al., 1986) is used and the ideal gas equation of state is employed in order to obtain the temperature.

The domain of calculation and its boundaries are illustrated schematically in Fig. 2, taking into account the axial symmetry of the problem. In the north boundary, the fluid properties are the same as the free-stream flow properties,

which were presented in Tab. 1. The west boundary is located on the symmetry line, so impermeability conditions are taken, that is, there is no flow of heat or fluid in the normal directions n to the contour. These conditions imply in

$$\frac{\partial u}{\partial n} = 0, \quad v = 0, \quad \frac{\partial p}{\partial n} = 0, \quad \frac{\partial T}{\partial n} = 0 \tag{3}$$

where T is the temperature. In the south boundary, slip condition and an adiabatic wall (without heat exchange) condition are taken, because in this work the flow is treated as inviscid, thus

$$\mathbf{n} \cdot \mathbf{v} = 0, \quad \frac{\partial p}{\partial n} = 0, \quad \frac{\partial T}{\partial n} = 0 \tag{4}$$

where the first term indicates that the velocity vector **v** is perpendicular to the normal vector **n**, that is, it is parallel to the cone surface. Finally, for the east boundary, which represents the outflow, the conditions are extrapolated from the upstream properties, because in supersonic flows the properties do not propagate in the opposite direction to the flow. In this way, it can be used

$$\frac{\partial u}{\partial x} = 0, \quad \frac{\partial v}{\partial x} = 0, \quad \frac{\partial p}{\partial x} = 0, \quad \frac{\partial T}{\partial x} = 0 \tag{5}$$

where x represents the axial direction.

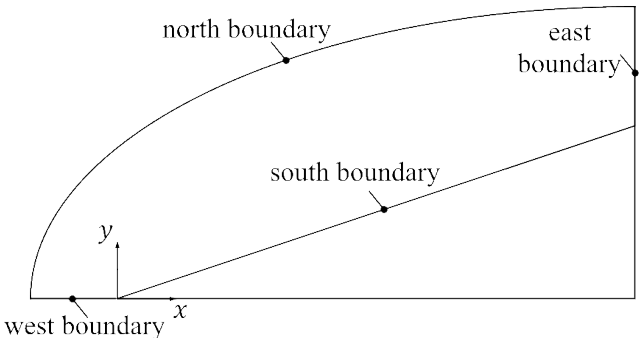

Figure 2. Illustration of the calculation domain and its boundaries.

The variable of interest used in this work is the drag coefficient (C_D), which is a dimensionless number used to quantify the drag on an object due to fluid flow. This coefficient is mathematically expressed for inviscid flows as

$$C_D = \frac{1}{0.5\,\rho_\infty u_\infty^2 A_T} \int_S (p - p_\infty) \cos\theta_n \, dA \tag{6}$$

where ρ_∞ is the density of the fluid, u_∞ and p_∞ are its velocity and pressure, respectively. These properties are from the free-stream flow. A_T is the area of the body transverse to the flow direction, p indicates the pressure along its surface S and θ_n is the angle between the normal of a surface area element and the flow direction. The drag coefficient is calculated numerically by approximating the integral of Eq. (6) using the Trapezoidal Rule.

Furthermore, a quadratic polynomial extrapolation method will be applied in an attempt to improve the pressure distribution on the cone surface and, hence, the drag coefficient. For the extrapolations, the Lagrange polynomial reads as

$$p_W = \frac{(0-d_2)(0-d_3)}{(d_1-d_2)(d_1-d_3)} p_1 + \frac{(0-d_1)(0-d_3)}{(d_2-d_1)(d_2-d_3)} p_2 + \frac{(0-d_1)(0-d_2)}{(d_3-d_1)(d_3-d_2)} p_3 \tag{7}$$

where the wall pressure p_W is calculated using the pressures p_1, p_2 and p_3. Points 1, 2, and 3 are the neighboring points inside the domain, where d is the distance of each point from the vertex of the surface control volume.

2.2 Verification and validation

Verification is a procedure used to assess the accuracy of a numerical simulation, indicating how close the numerical solution is to the analytical solution of the model. Validation is a procedure to assess the accuracy of the model compared

to the result of the real phenomenon. The difference between the numerical solution ϕ and the exact analytical solution Φ is the numerical error E_n (Ferziger et al., 2020)

$$E_n(\phi) = \Phi - \phi \tag{8}$$

The numerical error is mainly caused by the truncation errors E_h, iteration errors E_i and round-off errors E_π (Roache, 2009). In this work, iteration errors were minimized by maintaining iterative processes until they reached twice the number of iterations required for the residue of the system of mass conservation equations to be less than or equal to $1 \cdot 10^{-14}$. Round-off errors were minimized by using double precision in the calculations.

The procedure for quantifying the numerical error is called Verification and it measures the numerical accuracy of a numerical solution, or, in other words, how well the mathematical model is solved numerically. Generally, the exact analytical solution of most real fluid dynamics problems is not known. Thus, an estimate U_n of the numerical error is performed using an estimate of the exact analytical solution ϕ_∞

$$U_n = \phi_\infty - \phi \tag{9}$$

As in this work the round-off and iteration errors were minimized and, therefore, negligible, it is possible to obtain an estimate of the numerical error with *posteriori* procedures, which are performed after obtaining the numerical solution of the problem. This work will use the GCI estimator proposed by Roache (1994), the convergent estimator and convergent solution developed by Marchi (2001), and the RRE-based estimator and the solution extrapolated with RRE described by Martins (2013). For verification, the ASME V&V 20-2009 standard also recommends checking whether the apparent order (p_U), Eq. (10), converges to the theoretically expected value of the asymptotic order (p_0) of the discretization error. The standard recommends using at least four levels of mesh refinement for this analysis. The expected asymptotic order is two.

The apparent order is calculated using the numerical solutions ϕ of a fine mesh (ϕ_F), a coarse mesh (ϕ_C) and a supercoarse mesh (ϕ_{SC}), with constant refinement ratio r between them and equal to two, as follows

$$p_U = \frac{log\left(\left|\frac{\phi_C - \phi_{SC}}{\phi_F - \phi_C}\right|\right)}{log(r)} \tag{10}$$

Validation is the term used for the procedure of quantifying the modeling error (E_{model}) and it measures how well the mathematical model represents the physical phenomenon. The ASME V&V 20-2009 standard defines two metrics for the estimation of the modeling error: the comparison error (E) and the validation standard uncertainty (U_{val}), related to the modeling error by

$$E - U_{val} \leq E_{model} \leq E + U_{val} \tag{11}$$

Therefore, the modeling error is contained in the range of uncertainty given by $E \pm U_{val}$. The comparison error E is calculated by the difference between the numerical solution (ϕ) and the experimental result (X) of the problem, i.e.

$$E = \phi - X \tag{12}$$

The metric U_{val} is calculated by

$$U_{val} = \sqrt{U_{num}^2 + U_{input}^2 + U_{exp}^2} \tag{13}$$

where U_{num} is the standard numerical uncertainty, U_{input} is the standard uncertainty of the simulation input data and U_{exp} is the standard uncertainty of the experimental error. U_{num} is calculated, according to the ASME V&V 20-2009 standard, using the numerical error uncertainty U_{GCI} of the GCI estimator (Roache, 1994) as follows

$$U_{num} = \frac{U_{GCI}}{k},\ 1.1 \leq k \leq 1.15 \tag{14}$$

where k is called an expansion factor. In Eq. (13), it is considered that the uncertainties are independent of each other, but the ASME V&V 20-2009 standard also presents the procedure in case they are dependent. In addition, the standard presents the procedure for calculating the uncertainty U_{input}.

In order to perform the numerical error estimates, it is necessary to solve the same problem in meshes with different levels of refinement. For this, eight non-orthogonal meshes were generated with constant refinement equal to two and

simultaneous in each direction of the mesh. Figure 3 shows the initial mesh, which contains 20 control volumes in the main flow direction and 20 in the perpendicular direction. The meshes were generated using the GMSH code version 4.5.6 (Geuzaine and Remacle, 2009) and each of them was simulated in the SU2 code version 7.0.6 with multiprocessing support for the conditions of inviscid and axisymmetric flow. A computer with a processor Intel Core i7-6700 of 4.0 GHz, 32 GB of RAM and Debian operational system was employed for the simulations.

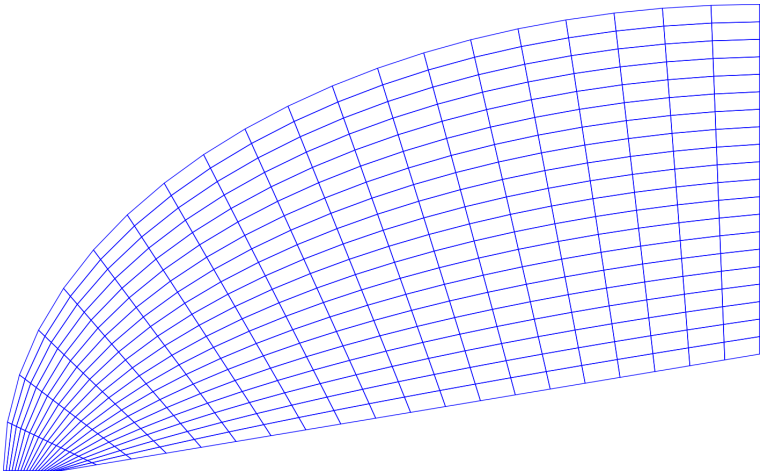

Figure 3. Initial mesh with 20x20 control volumes.

The drag coefficients obtained numerically were compared with the drag coefficient calculated from the numerical solution, with quadruple precision, of the Taylor-Maccoll irrotational flow (Taylor and Maccoll, 1933), which for the flow properties presented in Tab. 1 has the value of

$$C_D = 0.0754798301 \tag{15}$$

Besides the analysis of the apparent order, the ASME V&V 20-2009 standard recommends the comparison of the numerical solutions with those obtained by other authors. Therefore, the values of the drag coefficients obtained were compared with that of Bertoldo and Marchi (2017), who solved the same problem using the mathematical model of Euler in another computational code and the obtained value was

$$C_D = 0.075481 \pm 0.000006 \tag{16}$$

The estimated numerical error presented in Eq. (16) was calculated using the convergent estimator (Marchi and Silva, 2002). The numerical solution obtained by these authors went through verification procedures and the mathematical model by validation (Bertoldo and Marchi, 2017).

In order to validate the Euler's mathematical model, comparisons were made with the experimental result by Eggers Junior et al. (1957). As the authors only presented this experimental result graphically, the code WebPlotDigitizer 4.2 (Marin et al., 2017) was used to obtain the value of the drag coefficient from the graph. Hence, the value of the drag coefficient with uncertainty estimate considering the uncertainty due to the reading of the values in the graph (U_{read}) and the experimental uncertainty (U_{exp}) is

$$C_D = 0.0810 \pm 0.0019 \tag{17}$$

3. RESULTS AND DISCUSSION

This section presents the results and discussions of the results obtained. In the first subsection, the results of the verification and validation are presented. In the second subsection, the drag coefficients' results using extrapolated wall pressures are presented and comparisons with reference values are performed.

3.1 Verification and validation

The general results of the simulations performed with the SU2 code are presented in Tab. 2. This table contains the nomenclature of the meshes, as well as the number of volumes in each direction of the mesh, where N_x corresponds to the number of volumes along the main flow direction and N_y is the number of volumes in the direction perpendicular to the main flow direction. "Iterations" indicates the number of iterations required to complete the simulation, "Time" means

the simulation elapsed time, "RAM" is peak RAM memory usage of each simulation and C_D is the calculated drag coefficient. The apparent order p_U presented in Tab. 2 was calculated using Eq. (10), which uses the result of three meshes for its calculation. Figure 4 shows the Mach number field for the mesh m_8. The p_U values are close to two for the coarser meshes, which is the expected value of the asymptotic order and a decreasing behavior of the value of the apparent order is observed with the refinement of the mesh. The differences between the asymptotic order and the tendency of the apparent order may be, among other reasons, due to the high gradient of properties at the cone tip and also due to the shock wave formed, as can be seen in Fig. 4. The shock wave causes the order of accuracy downstream of the shock wave to reduce to the first order of accuracy in finer meshes (Roy, 2005; Carpenter and Casper, 1999).

Table 2. Simulation results.

Case	N_x	N_y	Iterations	Time	RAM (MB)	C_D	p_U
m_1	20	20	368	0.44 s	25.33	0.0732024777	-
m_2	40	40	446	1.04 s	31.33	0.0748019950	-
m_3	80	80	490	4.94 s	54.89	0.0752888900	1.72
m_4	160	160	724	43.59 s	142.54	0.0754241649	1.85
m_5	320	320	1094	4.91 min	504.70	0.0754628704	1.81
m_6	640	640	1692	38.46 min	1946.25	0.0754742404	1.77
m_7	1280	1280	2700	3.95 h	7668.51	0.0754777771	1.68
m_8	2560	2560	4448	1.11 day	30560.40	0.0754789895	1.54

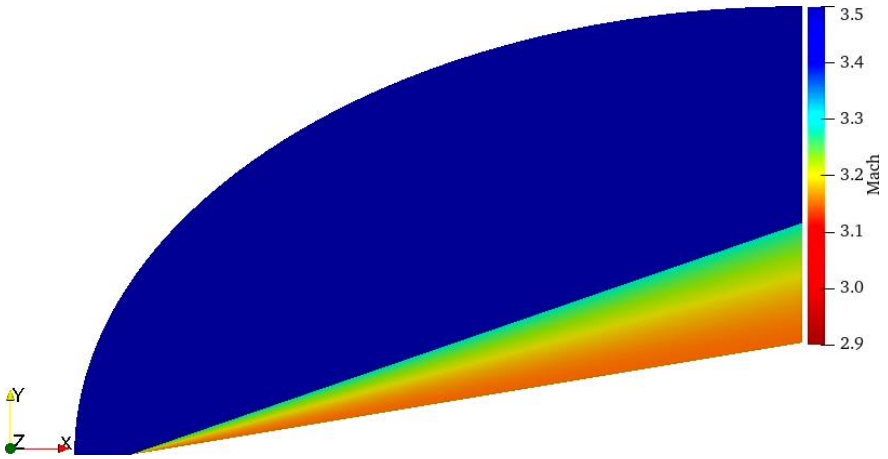

Figure 4. Mach number field of the finest mesh simulated.

The solution of the finest simulated mesh, extrapolated with RRE solution and convergent solution and their representations using the estimated numerical error are presented in Tab. 3. It can be noticed that the extrapolated solution with RRE is included in the interval given by the estimated error of the convergent solution, which is included in the estimated uncertainty obtained with the GCI estimator.

Table 3. Extrapolated and finest mesh solutions and their estimated numerical errors.

Method	C_D	Estimated error	Representation
GCI	0.0754789895	1.515522E-06	0.0754790 ± 0.0000015
Convergent	0.0754799119	2.899888E-07	0.07547991 ± 0.00000029
RRE	0.0754798250	-1.717229E-08	0.075479825 – 0.000000017

Table 4 presents the absolute values of the differences between the numerical solution of the Taylor-Maccoll flow and the solutions obtained from the simulations, which used Euler's mathematical model. The numerical solutions present increasing proximity to the numerical solution of the Taylor-Maccoll flow when refining the mesh. However, equality between the values obtained is not expected due to differences between the Euler mathematical model and the Taylor-Maccoll mathematical model. Figure 5 shows the pressure coefficients C_p of the cone surface of the Taylor-Maccoll solution, the numerical solution of the finest mesh and their absolute difference. Pressure coefficients are used in calculating the drag coefficient. The most significant difference is found at the tip of the cone, which results from different pressure values obtained by the two mathematical models. The simulation using Euler's mathematical model resulted in

a higher pressure coefficient followed by a drop and a subsequent stabilization along the cone surface. Perhaps meshes more refined at the cone tip would result in values even closer to the Taylor-Maccoll model.

Table 4. Comparisons of the values obtained from the simulations with the Taylor-Maccoll drag coefficient.

Case	C_D	Difference	Relative difference
m_1	0.0732024777	2.28E-03	3.02%
m_2	0.0748019950	6.78E-04	0.898%
m_3	0.0752888900	1.91E-04	0.253%
m_4	0.0754241649	5.57E-05	0.0737%
m_5	0.0754628704	1.70E-05	0.0225%
m_6	0.0754742404	5.59E-06	0.00741%
m_7	0.0754777771	2.05E-06	0.00272%
m_8	0.0754789895	8.41E-07	0.00111%

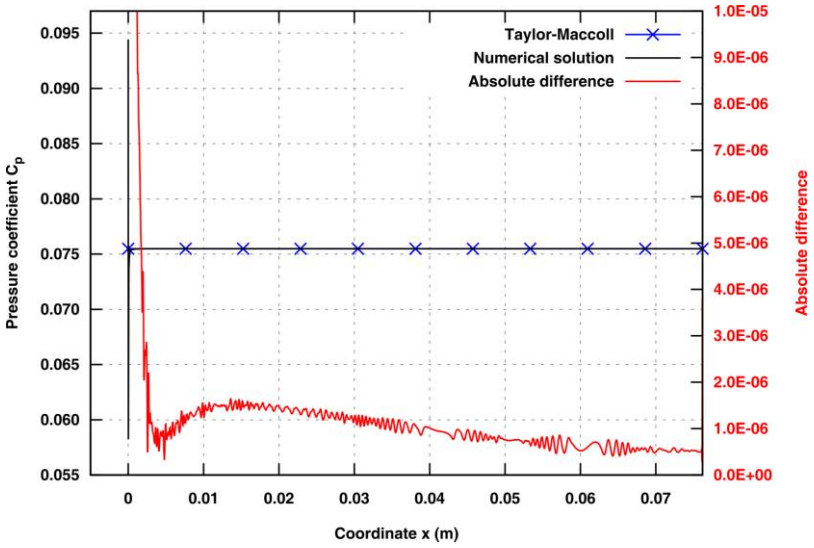

Figure 5. Pressure coefficients on the cone surface of the finest mesh simulated and of the Taylor-Maccoll solution.

Table 5 shows the absolute values of the differences between the solutions obtained from the simulations and the numerical drag coefficient obtained by Bertoldo and Marchi (2017), who also used Euler's mathematical model. It is observed that the differences between the solutions reduce with the refinement of the mesh and that the difference between the solution of the finest mesh and the solution of Bertoldo and Marchi (2017) is close to the estimated numerical error of the GCI estimator. Besides that, the numerical solution obtained in the finest mesh, m_8, is within the range of possible values given by the Bertoldo and Marchi's (2017) solution.

Table 5. Comparisons of the values obtained from the simulations with the numerical drag coefficient of Bertoldo and Marchi.

Case	C_D	Difference	Relative difference
m_1	0.0732024777	2.28E-03	3.02%
m_2	0.0748019950	6.79E-04	0.900%
m_3	0.0752888900	1.92E-04	0.255%
m_4	0.0754241649	5.68E-05	0.0753%
m_5	0.0754628704	1.81E-05	0.0240%
m_6	0.0754742404	6.76E-06	0.00896%
m_7	0.0754777771	3.22E-06	0.00427%
m_8	0.0754789895	2.01E-06	0.00266%

Comparisons with the experimental drag coefficient (Eggers Junior et al., 1957) are shown in Tab. 6. It can be noticed that the comparison error, calculated with Eq. (12), reduces as the mesh is refined, but its relative difference is still above 6.8%. As the experimental result contains an experimental uncertainty of ± 0.0019, the experimental value ranges from 0.0791 to 0.0829. Therefore, when comparing the simulations' results with the lowest value of the experimental drag

coefficient, 0.0791, the differences are reduced. For the meshes m_7 and m_8, relative differences of 4.579% and 4.578% are obtained, respectively. It should be remembered that in the experimental result there is the presence of viscous effects, which add a viscous portion to the drag coefficient, and that these effects are neglected by Euler's mathematical model.

Table 6. Comparisons of the values obtained from the simulations with the experimental drag coefficient.

Case	C_D	Comparison error	Relative difference
m_1	0.0732024777	-7.80E-03	9.63%
m_2	0.0748019950	-6.20E-03	7.65%
m_3	0.0752888900	-5.71E-03	7.05%
m_4	0.0754241649	-5.58E-03	6.88%
m_5	0.0754628704	-5.54E-03	6.84%
m_6	0.0754742404	-5.53E-03	6.82%
m_7	0.0754777771	-5.522E-03	6.818%
m_8	0.0754789895	-5.521E-03	6.816%

The standard uncertainty of the simulation input data U_{input} was calculated according to the ASME V&V 20-2009 standard, in which uncertainties were considered in the free-stream Mach number, free-stream temperature and fineness ratio (uncertainty due to the propagation of uncertainties of the length and diameter measures). These considerations resulted in U_{input} equal to 0.00039.

The validation metric U_{val} was calculated considering the standard numerical uncertainty given by the estimated numerical error of the GCI estimator of the finest mesh simulated, m_8, with an expansion factor equal to 1.1, the experimental uncertainty presented in Eq. (17) and the standard uncertainty of the simulation input data equals to 0.00039. Its value corresponds to

$$U_{val} = 0.0019 \tag{18}$$

It can be noticed that the validation standard uncertainty (U_{val}) was dominated by experimental uncertainty. Using the validation metrics U_{val} and E calculated for the finest mesh simulated, m_8, it is possible to use the Eq. (11) to conclude that the modeling error is contained in the range of $-7.42E\text{-}03 \leq E_{model} \leq -3.62E\text{-}03$. Comparing the magnitude of the validation metrics, U_{val} and E, it is noted that the comparison error (E) is approximately three times greater than the validation standard uncertainty (U_{val}). This indicates that the simplifications in Euler's mathematical model are the main sources of the modeling error.

3.2 Drag coefficients using extrapolated wall pressures

Table 7 presents the values of the drag coefficients calculated using extrapolated wall pressure distribution by means of quadratic polynomial extrapolation, Eq. (7), and the apparent orders. The apparent order has increasing value as the mesh is refined and it tends to a value greater than two. It is noticed the increase of the apparent order in relation to the values presented in Tab. 2, except for the value obtained in the mesh m_3. Regarding the drag coefficient, it is noted that it presents a decreasing behavior with the refinement of the mesh, which contrasts with the observed behavior when extrapolation is not applied.

Table 7. Drag coefficients using polynomial extrapolated wall pressures and apparent order.

Case	C_D	p_U
m_1	0.0783430861	-
m_2	0.0772607284	-
m_3	0.0758726206	-0.359
m_4	0.0755604912	2.15
m_5	0.0754949108	2.25
m_6	0.0754819255	2.34
m_7	0.0754796527	2.51
m_8	0.0754794524	3.50

The solution obtained from the finest simulated mesh, extrapolated with RRE solution and convergent solution and their representations using the estimated numerical error are presented in Tab. 8. The estimated numerical errors are lower than the ones obtained with the same estimators shown in Tab. 3, for the RRE, it is two orders of magnitude lower than the result without extrapolation of the pressure.

Table 8. Extrapolated and finest mesh solutions and their estimated numerical errors for the case where extrapolated wall pressures are used.

Method	C_D	Estimated error	Representation
GCI	0.0754794524	2.502900E-07	0.07547945 ± 0.00000025
Convergent	0.0754793427	9.044405E-08	0.075479343 ± 0.000000090
RRE	0.07547982564	-2.017986E-10	0.07547982564 – 0.00000000020

Table 9 shows comparisons to the Taylor-Maccoll drag coefficient and to the drag coefficient of Bertoldo and Marchi (2017). Regarding the comparisons with the Taylor-Maccoll solution, one can notice that the differences in the last four meshes are lower than the ones obtained without extrapolation of the wall pressure distribution, presented in Tab. 4. The same behavior occurred in the comparisons with the result of Bertoldo and Marchi (2017). No significant difference was observed in the comparisons in relation to the experimental value.

Table 9. Comparisons of the drag coefficients using polynomial extrapolated wall pressure distribution with the drag coefficients of Taylor-Maccoll and Bertoldo and Marchi.

Case	C_D	Difference Taylor-Maccoll	Relative difference Taylor-Maccoll	Difference Bertoldo and Marchi	Relative difference Bertoldo and Marchi
m_1	0.0783430861	2.86E-03	3.79%	2.86E-03	3.79%
m_2	0.0772607284	1.78E-03	2.36%	1.78E-03	2.36%
m_3	0.0758726206	3.93E-04	0.520%	3.92E-04	0.519%
m_4	0.0755604912	8.07E-05	0.107%	7.95E-05	0.105%
m_5	0.0754949108	1.51E-05	0.0200%	1.39E-05	0.0184%
m_6	0.0754819255	2.10E-06	0.00278%	9.26E-07	0.00123%
m_7	0.0754796527	1.77E-07	0.000235%	1.35E-06	0.00178%
m_8	0.0754794524	3.78E-07	0.000500%	1.55E-06	0.00205%

4. CONCLUSION

The study concluded that the comparison of numerical solutions with reference values is not enough to make statements about the quality of a mathematical model or a numerical model, being necessary to know quantitatively the estimated numerical error of a numerical solution. In this work, the drag coefficients calculated numerically were compared with the drag coefficient calculated according to the Taylor-Maccoll mathematical model, with the drag coefficient calculated with the same mathematical model by another computational code already verified and with an experimental result. The results indicate the proximity of the numerical solutions to the reference values with the refinement of the mesh. For the most refined simulated mesh, relative differences of 0.00111% were obtained in relation to the drag coefficient of the Taylor-Maccoll mathematical model and 0.00266% to the result obtained with the same mathematical model by another computational code. With the GCI estimator, it was obtained that the numerical error of the drag coefficient of the finest simulated mesh does not exceed 0.002% of its value. The smallest estimate was given by the RRE-based estimator, which corresponds to a range of 0.00002% of the RRE extrapolated solution. Finally, it was calculated that the modeling error due to the use of Euler's mathematical model to represent the physical phenomenon is contained in the range of -9.16% to -4.47% of the experimental result. About the drag coefficients calculated using extrapolated wall pressures by means of quadratic polynomial extrapolation, it was observed an increase in the apparent order and a reduction in the estimated numerical errors given by the error estimators, reaching a decrease of two orders of magnitude in the RRE-based estimator. Furthermore, the differences in relation to reference values became smaller when using extrapolated wall pressure distribution.

5. ACKNOWLEDGEMENTS

The authors acknowledge the Postgraduate Program in Mechanical Engineering (PGMEC) of Federal University of Paraná (UFPR) and the Conselho Nacional de Desenvolvimento Científico e Tecnológico (CNPq) for physical and financial support given for this work. This study was financed in part by the Coordenação de Aperfeiçoamento de Pessoal de Nível Superior (CAPES), Finance Code 001. Dener A. Iorio is supported by a CAPES scholarship. Carlos H. Marchi is supported by a CNPq scholarship. The first author also acknowledges Giovanne Deni Iorio for the support given in the development of the computational codes used in this work and their usage.

6. REFERENCES

ASME V&V 20–2009, 2009. *Standard for Verification and Validation in Computational Fluid Dynamics and Heat Transfer*. ASME, New York, United States of America.

Becker, G. G. and Granzoto, R. M., 2018. "DPW-6 and HiLiftPW-3 using the Stanford University Unstructured (SU2)". In *Proceedings of the 36th Applied Aerodynamics Conference* – AIAA Aviation Forum 2018. Atlanta, United States of America.

Bertoldo, G. and Marchi, C. H., 2017. "Verification and validation of the foredrag coefficient for supersonic and hypersonic flow of air over a cone of fineness ratio 3". *Applied Mathematical Modelling*, Vol. 44, pp. 409-424.

Carpenter, M. H. and Casper, J. H., 1999. "Accuracy of shock capturing in two spatial dimensions". *AIAA Journal*, Vol. 37, No. 9, pp. 1072-1079.

Castro, Í. C., 2019. *Assessment of SU2 for radial compressor performance prediction*. Master's thesis, Delft University of Technology, Delft, Netherlands.

Economon, T. D., Palacios, F., Copeland, S. R., Lukaczyk, T. W. and Alonso, J., 2016. "SU2: an open-source suite for multiphysics simulation and design". *AIAA Journal*, Vol. 54, No. 3, pp. 828-846.

Eggers Junior, A. J., Resnikoff, M. M. and Dennis, D. H., 1957. "Bodies of revolution having minimum drag at high supersonic airspeeds". *National Advisory Committee for Aeronautics*, Report 1306.

Ferziger, J. H., Perić, M. and Street, R. L., 2020. *Computational methods for fluid dynamics*. Springer, Zug, 4th edition.

Geuzaine, C. and Remacle, J. F., 2009. "Gmsh: a three-dimensional finite element mesh generator with built-in pre- and post-processing facilities". *International Journal for Numerical Methods in Engineering*, Vol. 79, No. 11, pp. 1309-1331.

Hirsch, C., 2007. *Numerical computation of internal and external flows: fundamentals of computational fluid dynamics*. Elsevier, Oxford, 2nd edition.

Hughes, T. J. R., Franca, L. P. and Mallet, M., 1986. "A new finite element formulation for computational fluid dynamics: I. Symmetric forms of the compressible Euler and Navier-Stokes equations and the second law of thermodynamics". *Computer Methods in Applied Mechanics and Engineering*, Vol. 54, No. 2, pp. 223-234.

Keep, J. A., Vitale, S., Pini, M. and Burigana, M., 2017. "Preliminary verification of the open-source CFD solver SU2 for radial-inflow turbine applications". *Energy Procedia*, Vol. 129, pp. 1071-1077.

Marchi, C. H., 2001. *Verificação de soluções numéricas unidimensionais em dinâmica dos fluidos*. Ph.D. thesis, Universidade Federal de Santa Catarina, Florianópolis, Brazil.

Marchi, C. H., Novak, L. A., Santiago, C. D. and Vargas, A. P. S, 2013. "Highly accurate numerical solutions with Repeated Richardson Extrapolation for 2D Laplace equation". *Applied Mathematical Modelling*, Vol. 37, No. 12-13, pp. 7386-7397.

Marchi, C. H. and Silva, A. F. C., 2002, "Unidimensional numerical solution error estimation for convergent apparent order". *Numerical Heat Transfer*, Part B, Vol. 42, No. 2, pp. 167-188.

Marin, F., Rohatgi, A. and Charlot, S., 2017. "WebPlotDigitizer, a polyvalent and free software to extract spectra from old astronomical publications: application to ultraviolet spectropolarimetry". *French Society of Astronomy & Astrophysics*.

Martins, M. A., 2013. *Multiextrapolação de Richardson com interpolação para reduzir e estimar o erro de discretização em CFD*. Ph.D. thesis, Universidade Federal do Paraná, Curitiba, Brazil.

Mishra, A. A., Mukhopadhaya, J., Iaccarino, G. and Alonso, J. J., 2019. "Uncertainty estimation of turbulence model predictions in SU2". *AIAA Journal*, Vol. 57, No. 3, pp. 1066-1077.

Palacios, F., Economon, T. D., Aranake, A. C., Copeland, S. R., Lonkar, A. K., Lukaczyk, T. W., Manosalvas, D. E., Naik, K. R., Padrón, A. S., Tracey, B., Variyar, A. and Alonso, J. J., 2014. "Stanford University Unstructured (SU2): open-source analysis and design technology for turbulent flows". In *Proceedings of the 52nd Aerospace Science Meeting* - AIAA SciTech Forum 2014. National Harbor, United States of America.

Roache, P. J., 1994. "Perspective: a method for uniform reporting of grid refinement studies". *ASME Journal of Fluids Engineering*, Vol. 116, No. 3, pp. 405-413.

Roache, P. J., 2009. *Fundamentals of verification and validation*. Hermosa, Albuquerque.

Roy, C. J., 2005. "Review of code and solution verification procedures for computational simulation". *Journal of Computational Physics*, Vol. 205, No. 1, pp. 131-156.

Taylor, G. I. and Maccoll, J. W., 1933. "The air pressure on a cone moving at high speeds". *Proceedings of the Royal Society of London*, Series A, Vol. 139, No. 838, pp. 278-297.

Van der Weide, E. and Economon, T. D., 2019. "Accuracy verification by means of exact and manufactured solutions". In *Proceedings of the 4th SU2 Developers Meeting* - SU2 Foundation 2019. Varenna, Italy.

7. RESPONSIBILITY NOTICE

The authors are the only responsible for the printed material included in this paper.